Inorganic Chemistry

ARTICLE

pubs.acs.org/IC

Crystal Structure of Novel Ni−Zn Borides: First Observation of a Boron−Metal Nested Cage Unit: $B_{20}Ni_6$

Zahida P. Malik,[†] Oksana Sologub,[†] Andriy Grytsiv,[†] Gerald Giester,[‡] and Peter F. Rogl*[,†]

[†]Institute of Physical Chemistry, University of Vienna, Währingerstrasse 42, A-1090 Vienna, Austria

[‡]Institute of Mineralogy and Crystallography, University of Vienna, Althanstr. 14, A-1090 Vienna, Austria

Supporting Information

ABSTRACT: The crystal structures of three ternary Ni−Zn borides have been elucidated by means of X-ray single-crystal diffraction (XSC) and X-ray powder diffraction techniques (XPD) in combination with electron microprobe analyses (EMPA) defining the Ni/Zn ratio. $Ni_{21}Zn_2B_{24}$ crystallizes in a unique structure type (space group $I4/mmm$; a = 0.72103(1) nm and c = 1.42842(5) nm; R_F^2 = 0.017), which contains characteristic isolated cages of B_{20} units composed of two corrugated octogonal boron rings, which are linked at four positions via boron atoms. The B_{20} units appear to have eight-membered rings on all six faces like the faces of a cube. Each face is centered by a nickel atom. The six nickel atoms are arranged in the form of an octahedron nested within the B_{20} unit. Such a boron aggregation is unique and has never been encountered before in metal−boron chemistry. The crystal structure of $Ni_{12}ZnB_{8-x}$ (x = 0.43; space group $Cmca$, a = 1.05270(2) nm, b = 1.45236(3) nm, c = 1.45537(3) nm; R_F^2 = 0.028) adopts the structure type of $Ni_{12}AlB_8$ with finite zigzag chains of five boron atoms. The compound Ni_3ZnB_2 crystallizes in a unique structure type (space group $C2/m$, a = 0.95101(4) nm, b = 0.28921(4) nm, c = 0.84366(3) nm, β = 101.097(3)°, and R_F^2 = 0.020) characterized by B_4 zigzag chain fragments with B−B bond lengths of 0.183−0.185 nm. The Ni_3ZnB_2 structure is related to the Dy_3Ni_2 type.

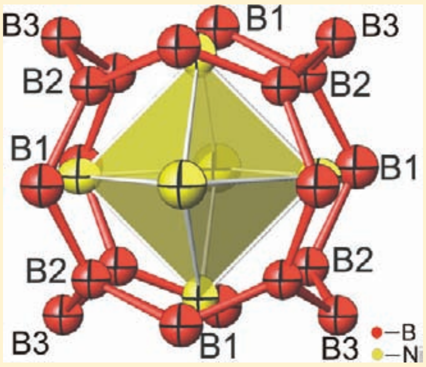

1. INTRODUCTION

The system Ce−Ni−Zn−B is part of the multinary Mg-based alloy system Mg−Zn−Mn(Ni)−RE used as high strength lightweight alloys for automotive applications (RE stands for a rare earth element).[1,2] Although little is yet known on the influence of nickel−boron additions in these multinary alloys, phase diagram information in terms of an isothermal section at 800 °C and a liquidus projection has been provided for the Ni-rich corner of the Ni−Zn−B subsystem by Stadelmaier et al.[3] The findings of Stadelmaier et al.[3−5] were used in a review of the Ni−Zn−B system by Bhan et al.[6] From the four ternary compounds identified,[3,4] only the crystal structure of the so-called τ phase of the $Cr_{23}C_6$ type ($Ni_{19.5}Zn_{3.5}B_6$) has been defined from X-ray powder and single crystal rotation photographs.[5] Metal borides are known to form a large variety of compounds, which are characterized by a large diversity of boron to boron bonds, reaching from isolated boron atoms in metal-rich compositions to boron clusters in "high"-boron compounds. On the basis of the classification of borides with respect to boron−boron aggregation as a function of the boron to metal ratio, B/M, boron clusters and frameworks have commonly been observed only at ratios B/M > 4 and comprise a quite large variety of regular and/or distorted boron clusters, cages, and frameworks such as (i) B_5-pentagonal pyramids in MgB_4,[7] (ii) B_4-square units connected by weak B−B bonds to a channel like framework in CrB_4[8] and MnB_4[9] hosting the metal atoms, (iii) B2 units connecting B_6 octahedra in Sm_2B_5[10] (Gd_2B_5[11]-type) borides, (iv) corner-connected boron octahedra B_6 in hexaborides forming a cage accepting large metal atoms,[12] (v) corner-linked B_{12} icosahedra through carbon atoms in $Mg_2B_{24}C$,[13] (vi) interconnected B_{12} cuboctahedra forming a B_{24} cage centered by metal atoms in dodecaborides,[14,15] (vii) eight supericosahedra $[B_{12}(B_{12})_{12}]$ per unit cell of the hectoborides MB_{66}[16,17] forming a framework that accepts metal atoms as well as additional borons. (viii) Icosahedra bonded via intericosahedral boron bonds create a series of structures such as MgB_7, $Mg_{\sim 5}B_{44}$,[18] and $MgAlB_{14}$.[19] (ix) Four icosahedra of boron atoms are linked by B−B bonds and carbon bridges in $AlB_{24}C_4$.[20] A linear C−B−C chain (B at the center of symmetry) links B_{12} icosahedra in $Al_{2.1}B_{51}C_8$.[21,22] The present work intends to elucidate the hitherto unknown crystal structures of the ternary Ni−Zn−B compounds.

2. EXPERIMENTAL SECTION

Samples at a total amount of ca. 1 g each were prepared from Ni foil (Alfa Aesar, purity >99.8 mass %), zinc granules (Alfa Aesar, purity >99.9 mass %), and boron pieces (ChemPur, Karlsruhe, purity 98 mass %). Zinc drops were purified in an evacuated quartz tube by heating them 50 °C below the boiling temperature of Zn (907 °C). Samples were prepared from intimate blends of powders of arc melted NiB_x master

Received: April 7, 2011
Published: July 19, 2011

alloys and fine Zn filings in proper compositional ratios. The blends were compacted at room temperature in a steel die without lubricants at a pressure of 800 MPa and were subsequently sealed in quartz tubes under vacuum conditions. Samples were heated to 1150 °C, kept at this temperature for 10 min, cooled to 800 °C at a rate of 1 °C/min, annealed at 800 °C for 7 days, and subsequently quenched in water.

X-ray powder diffraction data were collected from each alloy in as-cast and annealed states employing a Guinier−Huber image plate system with monochromatic Cu Kα1 radiation ($8° < 2\theta < 100°$). Quantitative Rietveld refinements of the X-ray powder diffraction data were performed with the FULLPROF program.[23]

Single crystals were mechanically isolated from crushed alloys. Inspections on an AXS-GADDS texture goniometer assured high crystal quality, unit cell dimensions, and Laue symmetry of the specimens prior to the X-ray intensity data collections on a four-circle Nonius Kappa diffractometer equipped with a CCD area detector employing graphite monochromated Mo Kα radiation (λ = 0.071069 nm). Orientation matrices and unit cell parameters were derived using the program DENZO.[24] No absorption corrections were performed because of the rather regular crystal shapes and small dimensions of the investigated specimens. The structures were solved by direct methods and were refined with the SHELXL-97 program[25,26] within the Windows version WINGX.[27]

The as-cast and annealed samples were polished using standard procedures, and microstructures and compositions were examined by light optical microscopy (LOM) and scanning electron microscopy (SEM) via electron probe micro-analyses (EPMA) on a Zeiss Supra 55 VP equipped with an EDX system operated at 20 kV. For Ni/Zn ratios, the binary compound Ni_2Zn_{11} at the Zn-rich boundary (15 at.% Ni[28]) was used as an EPMA standard. The differences between measured and nominal compositions were found to be less than ±1 atom %.

3. RESULTS AND DISCUSSION

3.1. Structural Chemistry. *3.1.1. Crystal Structure of $Ni_{21}Zn_2B_{24}$—A Novel Structure Type with a Metal Nested Cage, $B_{20}Ni_6$.* A single crystal suitable for X-ray structure determination was selected from the alloy $Ni_{30}Zn_{40}B_{30}$ (in atom %) annealed at 800 °C for 7 days. The observed extinctions are consistent with the body centered tetragonal space groups $I4$, $I\bar{4}$, $I4/m$, $I422$, $I4mm$, $I\bar{4}2m$, and $I4/mmm$. Structure solution was possible in space group $I\bar{4}2m$; however, the search for missing symmetry prompted the space group $I4/mmm$. Structure refinement in $I4/mmm$ resulted in seven fully occupied metal atom positions and three boron positions, yielding a structure formula $Ni_{21}Zn_2B_{24}$. With anisotropic atomic displacement parameters (ADPs) for the metal atoms and isotropic temperature factors for the boron sites, the final refinement converged to $R_F^2 = 0.017$ and residual electron densities smaller than ±1.62 $e^-/Å^3$. Structure data are summarized in Table 1, and the crystal structure is shown in Figures 1 and 2. The ratio Ni/Zn obtained from the refinement is 91.22:8.77, in good agreement with the ratio 91.0:9.0 derived from EPMA on the bulk sample. Rietveld refinement of the X-ray powder spectrum confirmed the structure model.

The crystal structure of $Ni_{21}Zn_2B_{24}$—shown in Figure 1a in three-dimensional view along [001]—is characterized by B_{20} units (Figure 1a,c,d) made of two eight-membered corrugated boron rings consisting of B1 and B2 atoms. Two such rings are linked at the four B2 positions via a B3 atom forming a B2−B3−B2 clamp and thereby building a cage around an empty Ni octahedron, $[Ni_6]$ (Figure 1d), which is nested within the B_{20} unit. The cage as well as the Ni octahedron is centered at site 2b (1/2,1/2,0). These cages appear to have eight-membered boron

Table 1. Structural Data for $Ni_{21}Zn_2B_{24}$

alloy composition (atom %)[a]	$Ni_{30}Zn_{40}B_{30}$
Ni/Zn atomic ratio, EPMA/refinement	91:9/91.2:8.8
formula from refinement	$Ni_{21}Zn_2B_{24}$
structure type	$Ni_{21}Zn_2B_{24}$
space group	$I4/mmm$; No. 139[b]
θ range; sets; frames; time/frame	$2.85 < \theta < 36.27$; 7; 403; 200 s
a [nm]	0.72103(1)
c [nm]	1.42842(5)
volume (nm^3)	74.261
Z	2
data collection/λ (nm)	Mo Kα radiation/0.071069
cryst size [μm]	20 × 30 × 45
mosaicity	0.59
reflns in refinement	493 $F_o > 4\sigma(F_o)$ of 561
number of variables	34
$R_F^2 = \Sigma\lvert F_o^2 - F_c^2\rvert/\Sigma F_o^2$	0.017
R_{Int}	0.064
GOF	0.685
extinction (Zachariasen)	0.00070(5)
Ni1 in 16n (0, y, z); occ.	y = 0.30020(5), z = 0.10062(3); 1.00(1)
U_{11};[c] U_{22}; U_{33}; U_{23}; $U_{13} = U_{12} = 0$	0.0042(2); 0.0059(2); 0.0063(2); −0.0010(1)
Ni2 in 8j (x, 1/2, 0); occ.	x = 0.24032(8); 1.00(1)
U_{11}; U_{22}; U_{33}; $U_{23} = U_{13} = U_{12} = 0$	0.0068(2); 0.0042(2); 0.0049(2)
Ni3 in 8f (1/4, 1/4, 1/4); occ.	1.00(1)
$U_{11} = U_{22}$; U_{33}; $U_{23} = U_{13}$; U_{12}	0.0113(2); 0.0053(2); −0.0003(1); 0.0051(2)
Ni4 in 4d (0, 1/2, 1/4); occ.	1.00(1)
$U_{11} = U_{22}$; U_{33}; $U_{23} = U_{13} = U_{12} = 0$	0.0048(2); 0.0043(3)
Ni5 in 2a (0, 0, 0); occ.	1.00(1)
$U_{11} = U_{22}$; U_{33}; $U_{23} = U_{13} = U_{12} = 0$	0.0034(2); 0.007(4)
Ni6 in 4e (0, 0, z); occ.	z = 0.36216(5); 1.00(1)
$U_{11} = U_{22}$; U_{33}; $U_{23} = U_{13} = U_{12} = 0$	0.0043(2); 0.0069(3)
Zn1 in 4e (0, 0, z); occ.	z = 0.19029(5); 1.00(1)
$U_{11} = U_{22}$; U_{33}; $U_{23} = U_{13} = U_{12} = 0$	0.0090(2); 0.0073(3)
B1 in 16n (0, y, z); occ.; U_{iso}[d]	y = 0.2984(4); z = 0.3453(2) 1.00(1); 0.0061(5)
B2 in 16m (x, x, z); occ.; U_{iso}	x = 0.2929(3), z = 0.1059(2) 1.00(1); 0.0052(5)
B3 in 16l (x, x, 0); occ.; U_{iso}	x = 0.2025(4); 1.00(1); 0.0052(6)
residual electron density; max; min in [electrons/nm^3] × 1000	1.62; −1.02

[a] Nominal composition of the alloy from which a single crystal was isolated. [b] Crystal structure data are standardized using the program Structure Tidy.[36] [c] Anisotropic atomic displacement parameters U_{ij} in [10^2 nm^2]. [d] Isotropic atomic displacement parameters U_{iso} in [10^2 nm^2].

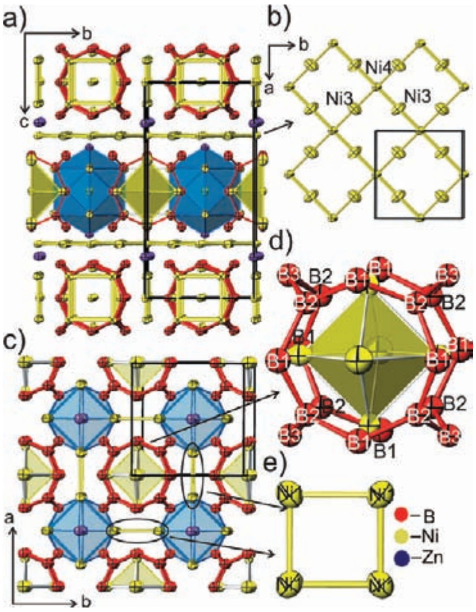

Figure 1. Crystal structure of $Ni_{21}Zn_2B_{24}$. (a) Perspective view along [100] with anisotropic displacement parameters (for metal atoms) from single crystal refinement. (b) Infinite Ni layer formed of −Ni3−Ni4−Ni3 atoms parallel to (001). (c) $Ni_{21}Zn_2B_{24}$ structure as an arrangement of (i) B_{20} units nesting empty octahedra [Ni_6] and (ii) Ni5[$Ni_8Zn_2B_4$] polyhedra (for better visualization, only the slab within $1/4 < z < 3/4$ is shown). (d) Enlarged view of B_{20} units in combination with empty octahedra [Ni_6]. (e) Ni_4 squares around the B_{20} unit.

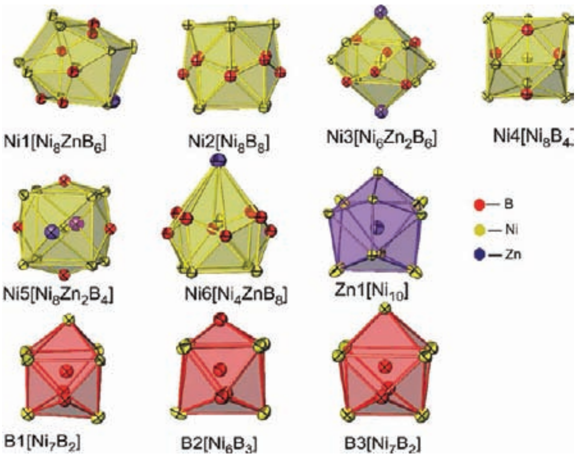

Figure 2. Coordination polyhedra of atoms in $Ni_{21}Zn_2B_{24}$.

rings on all six sides like the faces of a cube. The cages are stacked along [100] directly on top of each other. The boron−boron distances within the ring as well as the B2−B3 distances are within 0.177 nm of the sum of the covalent radii of two boron atoms (R_B = 0.088 nm). The distances between the center of the cage and the surrounding Ni atoms are d_{2b-Ni2} = 0.187 nm and d_{2b-Ni6} = 0.196 nm and are too short for metal−metal bonds.

It may be noted here that stabilities of hyper-coordinated d-block metal atoms centered in planar boron rings MB_n (n = 7, 8, 9, and 10) have recently been explored by density-function theory (DFT) computations.[29] Whereas the B_{20} units are flanked by squares of Ni1 atoms parallel to (100) and (010) (see Figure 1b), a square net formed by Ni3 and Ni4 atoms at a distance of 0.255 nm is attached to B1 (Ni4) and to B1 and B2 (Ni3). The unit cell contains two blocks of [Ni_6] nested B_{20} units, which are linked via B2−B3 bonds to a hexa-capped square prism around Ni5. These blocks are connected by shared infinite planar nets formed of intercrossed −Ni4−Ni3−Ni4− chains (Figure 1b). Along the z direction, the structure can be viewed as composed of Ni-atom chimneys, which accommodate the columns formed by alternating [Ni_6B_{20}] and Ni5[$Ni_8Zn_2B_4$] units (Figure 1c). The atomic environment for every atom site is depicted in Figure 2. Boron atoms are in tricapped trigonal prismatic coordination (CN = 9), in which we encounter seven metal atoms (B1 and B3) or six nearest metal neighbors (B2). Due to the smaller affinity of Zn to B with respect to Ni−B, the coordination figures around the boron atoms include only Ni atoms. The range of metal−boron distances from 0.199 to 0.228 is typical for nickel borides.[30] Metal atoms have coordination numbers ranging from 10 to 16, which in some cases form irregularly shaped coordination figures. For instance, the coordination polyhedron around the Ni2 atom is a slightly distorted Archimedian antiprism of metal atoms with a zigzag chain of eight boron atoms around its waist. Similarly, Zn is at the center of a bicapped Archimedian antiprism of metal atoms. Ni3 resides inside a hexa-capped square prism revealing distorted rhombic and triangular faces. The atomic environment of Ni4 is a distorted cuboctahedron. Ni5 is at the center of a square prism of eight Ni atoms, with the six faces capped by four B and two Zn atoms. Ni6 atoms reside in a basket formed by a square Ni atom base and a zigzag ring of eight boron atoms capped by a Zn atom. It should be emphasized that the B_{20} units are a unique boron aggregation that has never been encountered before in metal−boron chemistry.[31]

In view of boride classification, the crystal structure of $Ni_{21}Zn_2B_{24}$, although its boron/metal ratio is only slightly higher than 1, is a new example of the combination of a boron cage with a nested empty metal octahedron forming a $B_{20}Ni_6$ unit linking the electron deficient boron atoms in the cage to the metal framework of the crystal structure. It is somewhat surprising that the nested metal octahedron is formed by Ni atoms, which themselves need to fill their d shell. In order to fully elucidate this particularly interesting bonding situation, a current investigation focuses on the physicochemical properties of $Ni_{21}Zn_2B_{24}$ in combination with a DFT calculation of the electronic structure.

3.1.2. Crystal Structure of $Ni_{12}ZnB_{8-x}$ (x = 0.43) with $Ni_{12}AlB_8$ Structure Type. A single crystal was selected from a crushed as-cast sample, $Ni_{58.34}Zn_{4.86}B_{36.79}$ (in atom %). Systematic extinctions for a C-centered orthorhombic unit cell (a = 1.05270(2) nm, b = 1.45236(3) nm, and c = 1.45537(3) nm) resulted in two possible space group types, *C*2*cb* (standard setting *Aba*2) and *Cmca*. Structure solution with direct methods was successful in centrosymmetric *Cmca*, the space group of highest symmetry. Refinement—employing anisotropic atomic displacement parameters (ADPs) for the metal atoms and isotropic temperature factors for the boron atoms—converged to R_F^2 = 0.028 with residual electron densities less than ±2.0 $e^-/Å^3$. With Zn and Ni atoms in 13 independent and fully occupied positions and nine sites for boron atoms, of which the sites for B8 and B9 were occupied at 70% and 65%, respectively, the refinement yielded the composition $Ni_{12}ZnB_{8-x}$ (x = 0.43). The ratio Ni/Zn = 92.3:7.7 is in accordance with the value of 91.6:8.4 found by EPMA. Unit cell parameters, crystal symmetry, and atom distribution reveal isotypism with the structure type

Table 2. Structural Data for $Ni_{12}ZnB_{8-x}$ (x = 0.43)

alloy composition (atom %)[a]	$Ni_{58.34}Zn_{4.86}B_{36.79}$
Ni/Zn atomic ratio, EPMA/refinement	91.6:8.4/92.3:7.7
formula from refinement	$Ni_{12}ZnB_{8-x}$ (x = 0.43)
structure type	$Ni_{12}AlB_8$
space group	*Cmca*; No. 64 [b]
θ range; sets; frames; time/frame	$2.77 < \theta < 34.99$; 7; 516; 200 s/frame
a; b; c [nm]	1.05270(2); 1.45236(3); 1.45537(3)
volume (nm^3)	222.511(2)
Z	1
data collection/λ (nm)	Mo Kα radiation/0.071069
cryst size [μm]	25 × 30 × 40
mosaicity	0.48
reflns in refinement	$1823F_o > 4\sigma(F_o)$ of 2554
number of variables	129
$R_F^2 = \Sigma\lvert F_o^2 - F_c^2\rvert/\Sigma F_o^2$	0.028
R_{Int}	0.060
GOF	1.037
extinction (Zachariasen)	0.00017(1)
Ni1 in 8f (0, y, z); occ.	y = 0.42251(4), z = 0.08096(4); 1.00(1)
U_{11}; U_{22}; U_{33}; U_{23}; $U_{13} = U_{12} = 0$	0.0083(3); 0.0102(3); 0.0092(3); −0.0022(2)
Ni2 in 16g (x, y, z); occ.	x = 0.37254(5), y = 0.06824(3), z = 0.06440(3); 1.00(1)
U_{11};[c] U_{22}; U_{33}; U_{23}; U_{13}; U_{12}	0.0112(2); 0.0096(2); 0.0104(2); 0.0008(2); 0.0004(2); 0.0005(1)
Ni3 in 8f (0, y, z); occ.	y = 0.13668(4), z = 0.12413(4); 1.00(1)
U_{11}; U_{22}; U_{33}; U_{23}; $U_{13} = U_{12} = 0$	0.0092(3); 0.0081(3); 0.0074(3); 0.0007(2)
Ni4 in 16 g (x, y, z); occ.	x = 0.13373(4), y = 0.42087(3), z = 0.22086(3); 1.00(1)
U_{11}; U_{22}; U_{33}; U_{23}; U_{13}; U_{12}	0.0087(2); 0.0099(2); 0.0075(2); −0.0006(2); −0.0003(2); 0.0014(2)
Ni5 in 16 g (x, y, z); occ.	x = 0.16955(4), y = 0.00959(3), z = 0.13227(3); 1.00(1)
U_{11}; U_{22}; U_{33}; U_{23}; U_{13}; U_{12}	0.0096(2); 0.0080(2); 0.0088(2); 0.0008(2); 0.0014(2); 0.0003(2)
Ni6 in 8f (0, y, z); occ.	y = 0.38296(4), z = 0.36934(4); 1.00(1)
U_{11}; $U_{22} = U_{33}$; U_{23}; $U_{13} = U_{12} = 0$	0.0089(3); 0.0078(3); −0.0002(2)
Ni7 in 16g (x, y, z); occ.	x = 0.16960(4), y = 0.13245(3), z = 0.00178(3); 1.00(1)
$U_{11} = U_{22}$; U_{33}; U_{23}; U_{13}; U_{12}	0.0096(2); 0.0088(2); 0.0017(2); 0.0005(2); 0.0015(2)
Ni8 in 16 g (x, y, z); occ.	x = 0.13588(4), y = 0.28315(3), z = 0.08587(3); 1.00(1)
U_{11}; U_{22}; U_{33}; U_{23}; U_{13}; U_{12}	0.0089(2); 0.0079(2); 0.0106(2); −0.00003(15); −0.0011(2); −0.0002(2)
Ni9 in 16g (x, y, z); occ.	x = 0.36810(4), y = 0.23615(3), z = 0.10344(3); 1.00(1)
U_{11}; U_{22}; U_{33}; U_{23}; U_{13}; U_{12}	0.0108(2); 0.0073(2); 0.0088(2); 0.0005(2); 0.0019(2); 0.0008(2)
Ni10 in 16g (x, y, z); occ.	x = 0.13440(4), y = 0.11128(3), z = 0.26854(3); 1.00(1)
U_{11}; U_{22}; U_{33}; U_{23}; U_{13}; U_{12}	0.0120(2); 0.0093(2); 0.0081(2); −0.0004(2); 0.0005(2); −0.0016(2)
Ni11 in 8e (1/4, y, 1/4); occ.	y = 0.26391(4); 1.00(1)
U_{11}; U_{22}; U_{33}; U_{13}; $U_{23} = U_{12} = 0$	0.0090(3); 0.0075(3); 0.0078(3); 0.00058(2)
Zn1 in 8f (0, y, z); occ.	y = 0.26794(4), z = 0.23828(4); 1.00(1)
U_{11}; U_{22}; U_{33}; U_{23}; $U_{13} = U_{12} = 0$	0.0098(3); 0.0111(3); 0.0117(3); −0.0025(2)
Zn2 in 4a (0, 0, 0); occ.	1.00(1)
U_{11}; $U_{22} = U_{33}$; U_{23}; $U_{13} = U_{12} = 0$	0.0097(4); 0.0096(4); 0.0011(3)
B1 in 8f (0, y, z); occ.; U_{iso}[d]	y = 0.0249(4), z = 0.3280(4); 1.00(1); 0.012(1)
B2 in 8f (0, y, z); occ.; U_{iso}	y = 0.0113(4), z = 0.2053(4); 1.00(1); 0.0082(10)
B3 in 16g (x, y, z); occ.; U_{iso}	x = 0.1906(4), y = 0.4256(3), z = 0.0792(3); 1.00(1); 0.0093(7)
B4 in 8f (0, y, z); occ.; U_{iso}	y = 0.1727(4), z = 0.4824(4); 1.00(1); 0.011(1)
B5 in 8f (0, y, z); occ.; U_{iso}	y = 0.2958(4), z = 0.4969(4); 1.00(1); 0.010(1)
B6 in 16g (x, y, z); occ.; U_{iso}	x = 0.2987(4), y = 0.3624(3), z = 0.1514(3); 1.00(1); 0.0092(7)
B7 in 16g (x, y, z); occ.; U_{iso}	x = 0.2115(4), y = 0.1546(3), z = 0.1426(3); 1.00(1); 0.0121(8)
B8 in 8d (x, 1/2, 0); occ.; U_{iso}	x = 0.2722(7); 0.70(2); 0.007(2)
B9 in 8f (0, y, z); occ.; U_{iso}	y = 0.1428(6), z = 0.3615(5); 0.65(2); 0.008(2)
residual electron density; max; min in [electrons/nm^3] × 1000	2.01; −1.49

[a] Nominal composition of the alloy from which a single crystal was isolated. [b] Crystal structure data are standardized using the program Structure Tidy.[36] [c] Anisotropic atomic displacement parameters U_{ij} in [10^2 nm^2]. [d] Isotropic atomic displacement parameters U_{iso} in [10^2 nm^2].

$Ni_{12}AlB_8$.[32] Crystallographic data including occupancy and thermal parameters for individual atomic positions are summarized in Table 2. Figure 3 portrays the crystal structure of $Ni_{12}ZnB_{8-x}$ in three-dimensional view along [100].

As described earlier,[32] the structure type of $Ni_{12}AlB_8$ is characterized by a stacking of two layer units alternating along [100]. Both layers are characterized by five-membered boron zigzag chains running along [011] and [01−1]. Whereas the boron zigzag orientation is in the *bc* plane for the layer at $x = 0$, the zigzag orientation for the layer $x = 0.5$ changes to the plane $a - b\sqrt{2}$. Besides the B−B chains, isolated boron atoms exist in the layer at $x = 0.5$.

B−B distances in the chain (B_6−B_3−B_8−B_3−B_6) parallel to the *bc* plane are uniformly 0.180 nm, but B−B distances in the chain (B_5−B_4−B_9−B_1−B_2) parallel to the $a - b\sqrt{2}$ plane range from 0.178 to 0.181 nm, all close to the sum of covalent boron radii. The site for B9 is occupied by 65% only and is further bonded to 6Ni + 1Zn + 2B. Whereas Ni1 centers a cube of eight Ni atoms capped by four boron atoms, Ni2 has a waist of boron atoms B3−B8−B3 and B1−B9−B4 (both from the middle part of two different five-membered zigzag chains); above and below are squares of metal atoms, one of which is capped by a B7 atom (isolated boron atom in the unit cell). Ni3, Ni6, and Ni11 are at the centers of a rather distorted cube with Ni atoms at eight corners, and all six faces are capped (by 2Zn + 4B atoms). Polyhedra of Ni4, Ni5, Ni7, Ni8, Ni9, and Ni10 form triangular and square faces with five boron and 10 metal atoms. Ni11 has 10 metal and four B atoms in its polyhedron. Zn1 and Zn2 reside in cuboctahedra with additional boron atoms. For Zn1, one square is capped by one B atom, while for Zn2, two boron atoms cap squares (see Figure 4a). For boron coordination, see Figure 4b. While B1, B3, B4, B8, and B9 form tricapped trigonal prisms bonding to two boron atoms at a total coordination number of 9, atoms B2, B5, B6, and B7 are inside square antiprisms, where one square face is capped by a boron atom for B2, B5, and B6 but by a metal atom in the case of B7. Isolated boron atoms (B7) in tetrakaidecahedral metal coordination in combination with boron chain fragments are consistent with the low boron to metal ratio in the structure (B/M = 8:13) as a typical feature seen in low-boron structure types.[3]

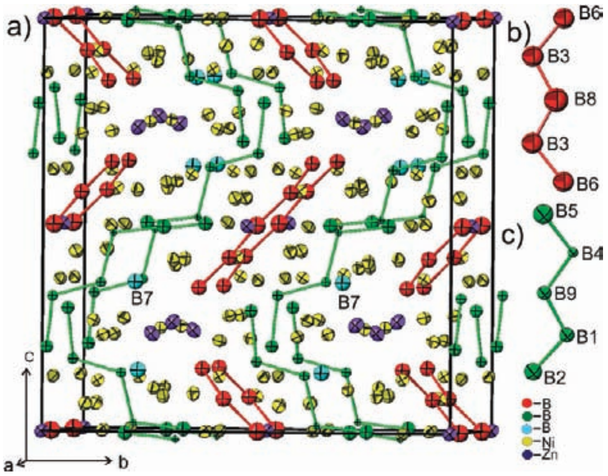

Figure 3. Unit cell of $Ni_{12}ZnB_{8-x}$ ($x = 0.43$), showing (a) two types of isolated five-membered boron zigzag chains, (b) a B6−B3−B8−B3−B6 chain with a B−B equidistance of 0.180 nm, and (c) a B5−B4−B9−B1−B2 chain with different B−B distances.

3.1.3. Crystal Structure of Ni_3ZnB_2—A Novel Structure Type. Single crystals of Ni_3ZnB_2 were grown from an alloy of composition $Ni_{23}Zn_{67}B_{10}$ (in atom %) melted at 1150 °C, slowly cooled at 0.5 °C/min to 970 °C, and water quenched. The excess of Zn was dissolved in dilute HCl. The observed extinctions are consistent with the C-centered monoclinic space groups *C*2/*m*, *C*2, and *Cm*. Structure refinement in *C*2/*m* resulted in four fully occupied metal atom positions and two boron positions, yielding a new and unique structure type, Ni_3ZnB_2. With anisotropic atomic displacement parameters (ADPs) for the metal atoms and isotropic temperature factors for the boron atoms, the final refinement converged to $R_F^2 = 0.020$ and residual electron

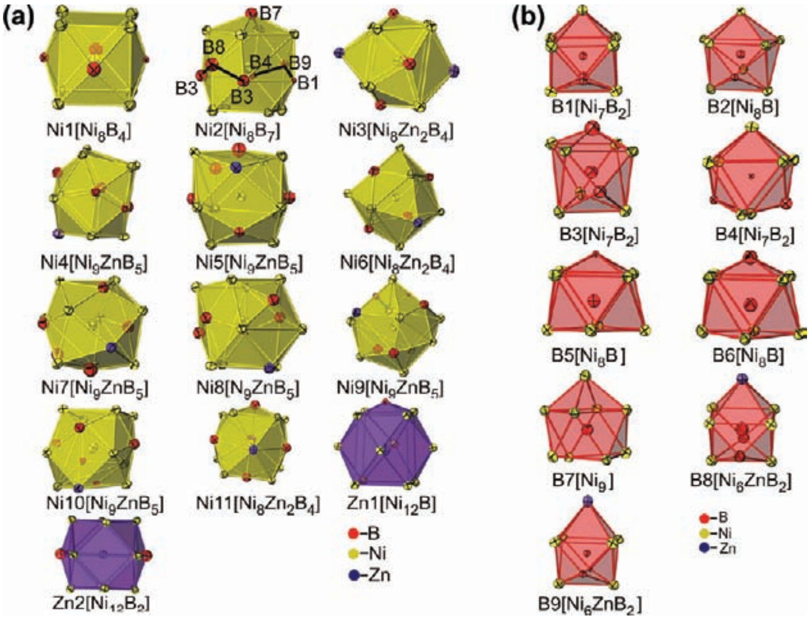

Figure 4. (a) Coordination polyhedra around Ni and Zn atoms in $Ni_{12}ZnB_{8-x}$ ($x = 0.43$). (b) Coordination polyhedra around B atoms in $Ni_{12}ZnB_{8-x}$ ($x = 0.43$).

Table 3. Crystal Structure Data for Ni_3ZnB_2

alloy composition (atom %)[a]	$Ni_{23}Zn_{67}B_{10}$
Ni/Zn atomic ratio, EPMA/refinement	75:25/75:25
formula from refinement	$Ni_{50}Zn_{16.66}B_{33.34}$
structure type	Ni_3ZnB_2
space group	$C2/m$; No. 12[b]
θ range [deg]; sets; frames; time/frame	$2.46 < \theta < 35.60$; 6, 335, 335 s/frame
a [nm]	0.95101(4)
b [nm]	0.2891(4)
c [nm]	0.84366(3)
β [deg]	101.097(3)
volume (nm^3)	22.77(3)
Z	4
data collection/λ (nm)	Mo Kα radiation/0.071069
cryst size [μm]	25 × 35 × 40
mosaicity	0.48
reflns in refinement	527 $F_o > 4\sigma(F_o)$ of 593
number of variables	34
$R_F^2 = \Sigma\lvert F_o^2 - F_c^2\rvert/\Sigma F_o^2$	0.020
R_{Int}	0.058
GOF	0.692
extinction (Zachariasen)	0.0129(7)
Ni1 in 4i (x, 0, z); occ.	$x = 0.21879(5)$, $z = 0.25127(6)$; 1.00(1)
U_{11}; U_{22}; U_{33}; U_{13}; $U_{23} = U_{12} = 0$	0.0041(2); 0.0058(2); 0.0041(2); 0.0008(1)
Ni2 in 4i (x, 0, z); occ.	$x = 0.49680(5)$, $z = 0.28968(6)$; 1.00(1)
U_{11}; U_{22}; U_{33}; U_{13}; $U_{23} = U_{12} = 0$	0.0049(2); 0.0053(2); 0.0051(2); 0.0013(1)
Ni3 in 4i (x, 0, z); occ.	$x = 0.63894(5)$, $z = 0.00305(6)$; 1.00(1)
U_{11}; U_{22}; U_{33}; U_{13}; $U_{23} = U_{12} = 0$	0.0050(2); 0.0052(2); 0.0049(2); 0.0008(1)
Zn1 in 4i (x, 0, z); occ.	$x = 0.13845(5)$, $z = 0.52534(5)$; 1.00(1)
U_{11}; U_{22}; U_{33}; U_{13}; $U_{23} = U_{12} = 0$	0.0068(2); 0.0080(2); 0.0045(2); 0.0013(1)
B1 in 4i (x, 0, z); occ.; U_{iso}[c]	$x = 0.1550(5)$, $z = 0.8151(5)$; 1.00(1); 0.0062(7)
B2 in 4i (x, 0, z); occ.; U_{iso}	$x = 0.0145(5)$, $z = 0.1119(5)$; 1.00(1); 0.0069(7)
residual electron density; max; min in [electrons/nm^3] × 1000	1.59; −1.33

[a] Nominal composition of the alloy from which a single crystal was isolated. [b] Crystal structure data are standardized using the program Structure Tidy.[36] [c] Isotropic atomic displacement parameters U_{iso} in [10^2 nm^2].

densities smaller than ±1.6 $e^-/Å^3$. X-rays cannot distinguish well between Ni and Zn because they differ by only two electrons; therefore, positions of Zn and Ni atoms in the unit cell have been defined with respect to interatomic distances. Structure data are summarized in Table 3. The Ni/Zn ratio obtained from the refinement is 75:25, in good agreement with the experimental ratio of 75:25 derived from EPMA on the bulk sample.

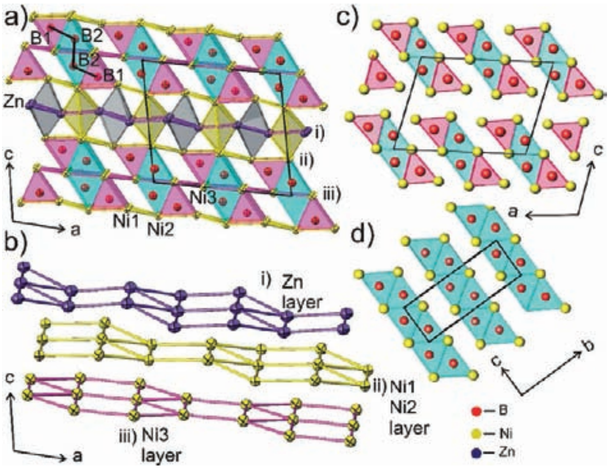

Figure 5. Crystal structure of Ni_3ZnB_2. (a) AlB_2-type fragments and four-membered zigzag chains of boron atoms with octahedra around (0,0, 1/2) and (3/4,3/4, 1/2). (b) Slightly puckered 3^34^2 layers of metal atoms. (c) Dy_3Ni_2 structure along the [010] projection with AlB_2-type fragments and four-membered zigzag chains of Ni atoms. (d) CrB structure along [100] with AlB_2-type fragments containing infinite zigzag chains of B atoms.

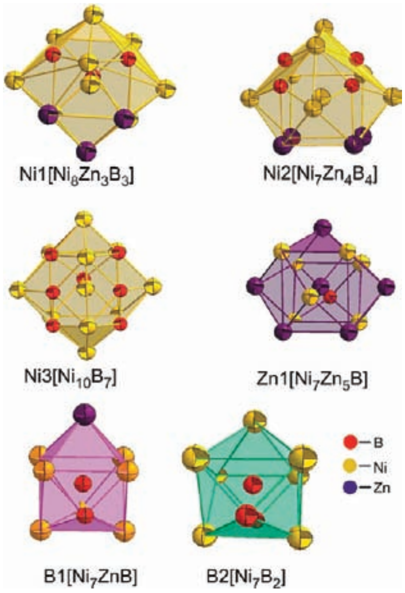

Figure 6. Coordination polyhedra for the Ni_3ZnB_2 structure.

Figure 5a shows the unit cell drawn along the b axis. Whereas Zn atoms form a continuous and slightly puckered 3^34^2 grid of triangles and rectangles (see Figure 5b), coupled triangular prisms around boron atoms resemble the AlB_2 structural fragments. Four face-connected triangular prisms form a B_4-zigzag chain unit (Figure 5a). The B−B distances ($d_{B1-B2} = 0.1833$ nm and $d_{B2-B2} = 0.1855$ nm) are consistent with the sum of B−B atomic radii. The same kinds of B4 units have been observed in the structure types of Mo_2IrB_2[33] and αCr_2IrB_2.[34] The coordination figures of all crystallographic sites are summarized in Figure 6. The polyhedron for the Zn site has one boron and 12 metal atoms in a distorted penta-capped square prism remotely reminiscent of the shape of a rhombododecahedron with one missing atom. The Ni1 atom has three boron and 11 metal atoms forming a distorted cube-octahedron. Ni2 has four boron and 11 metal atom neighbors, resulting in a polyhedron with triangular and square faces. The atom environment of Ni3 accounts for seven boron and 10 Ni atoms. B1 and B2 atoms center a tricapped prism (CN = 9, see Figure 6). The Ni_3ZnB_2 structure is related to Dy_3Ni_2,[35] where infinite columns of face-sharing monocaped triangular prisms $Ni[Dy_6]$ are running along the *b* direction. Both structures, Dy_3Ni_2 and Ni_3ZnB_2, originate from the CrB-type structure which in turn is an intergrowth structure of AlB_2 and W fragments consisting of infinite planar layers of face-connected triangular prisms alternating with the columns of face-linked empty tetrahedra and empty tetragonal pyramids. In the case of Ni_3ZnB_2, due to insertion of the puckered 3^34^2 layers of metal atoms, their rectangular prism faces are coupled by empty octahedra. The shortest distances between octahedral centers and metal ligands are only 0.13−0.14 nm, and therefore these voids are too small to accommodate any interstitial atom.

CONCLUSION

The crystal structures of three ternary Ni−Zn borides have been elucidated by means of X-ray single crystal and powder diffraction techniques assisted by electron microprobe analyses defining the Ni/Zn ratio. B−B bonds manifest unique structure formations in the Ni−Zn borides. The structure of $Ni_{21}Zn_2B_{24}$ is the first example of characteristic isolated cages of B_{20} units composed of two octogonal boron rings that are fused at four positions by boron atoms. All boron atoms are at a distance of 0.177 nm from one another. As a new feature, a Ni_6 octahedron is nested within the B_{20} cage. The crystal structure of $Ni_{12}ZnB_{8-x}$ ($x = 0.43$) is isotypic with $Ni_{12}AlB_8$ and reveals finite zigzag chains of five boron atoms. Ni_3ZnB_2 adopts a unique structure type with characteric B_4 zigzag chain fragments at a B−B bond distance of 0.180 nm.

ASSOCIATED CONTENT

Ⓢ **Supporting Information.** X-ray crystallographic file in CIF format, tables on interatomic distances. This material is available free of charge via the Internet at http://pubs.acs.org.

AUTHOR INFORMATION

Corresponding Author

*Tel.: +43 1 4277 52456. Fax: +43 1 4277 95245. E-mail: peter.franz.rogl@univie.ac.at.

ACKNOWLEDGMENT

The research reported herein was supported by the Higher Education Commission of Pakistan (HEC) under the scholarship scheme “PhD in Natural & Basic Sciences from Austria”. We thank to Dr. S. Puchegger for his expert assistance in EPMA measurements.

REFERENCES

(1) Moreno, I. P.; Nandy, T. K.; Jones, J. W.; Allison, J. E.; Pollock, T. M. *Scripta Mater.* **2003**, *48*, 1029–1034.

(2) Kang, Y.-B.; Pelton, A. D.; Chartrand, P.; Spencer, P.; Fuerst, C. D. *J. Phase Equilib. Diffusion* **2007**, *28*, 242.

(3) Stadelmaier, H. H.; Schöbel, J.-D.; Jordan, L. T. *Metall.* **1962**, *16*, 752–754.

(4) Stadelmaier, H. H.; Yun, T. S. *Z. Metallkde* **1962**, *53*, 754–756.

(5) Stadelmaier, H. H.; Draughn, R. A.; Hofer, G. *Z. Metallkde* **1963**, *54*, 640–644.

(6) Bhan, S.; Singh, S.; Lal, A. *J. Alloy Phase Diagrams (India)* **1990**, 3, 147–152.

(7) Guette, A.; Naslain, R.; Galy, J. C. R. *Acad. Sc. Paris* **1972**, *275*, 41–44.

(8) Andersson, S.; Lundström, T. *Acta Chem. Scand.* **1968**, *24*, 3101–3110.

(9) Andersson, S; Carlsson, J.-O. *Acta Chem. Scand.* **1970**, *22*, 1791–1799.

(10) Zavalii, L. V.; Kuz’ma, Y. B.; Mikhalenko, S. I. *Poroshkova Metallurgiya* **1990**, *6* (330), 61–63.

(11) Schwarz, S.; Simon, A. *Z. Naturforsch.* **1987**, *42b*, 935–939.

(12) Schell, S.; Winter, H.; Reitschel, H.; Gompf, F. *Phys. Rev. B* **1982**, *25*, 1589–1599.

(13) Adasch, V.; Hess, K.-U.; Ludwig, T.; Vojteer, N.; Hillebrecht, H. *J. Solid State Chem.* **2006**, *179*, 2150–2157.

(14) Leithe-Jasper, A.; Sato, A.; Tanaka., T. *Z. Kristallogr. NCS* **2002**, *217*, 319–320.

(15) Matkovich, V. I.; Economy, J.; Giese, R. F.; Barrett, R. *Acta Crystallogr.* **1965**, *19*, 1056–1058.

(16) Richards, S. M.; Kasper, J. S. *Acta Crystallogr.* **1969**, *B25*, 237–251.

(17) Perkins, C. L.; Trenary, M. *Phys. Rev. Lett.* **1996**, *77*, 1772–4775.

(18) Pediaditakis, A.; Schroeder, M.; Sagawe, V.; Ludwig, T.; Hillebrecht, H. *Inorg. Chem.* **2010**, *49*, 10882–10893.

(19) Matkovich, V. I.; Economy, J. *Acta Crystallogr.* **1970**, *B26*, 616–621.

(20) Will, V. G. *Acta Crystallogr.* **1969**, *B25*, 1219–1222.

(21) Perrotta, A. J.; Townes, W. D.; Potenza, J. A. *Acta Crystallogr.* **1969**, *B25*, 1223–1229.

(22) Meyer, F. D.; Hillebrecht, H. *High Temp. Mater. Chem., Pt. 1* **2000**, 161–164.

(23) Roisnel, T.; Rodriguez-Carvajal, J. *Mater. Sci. Forum* **2010**, *118*, 378–381.

(24) *Nonius Kappa CCD Program Package: COLLECT, DENZO, SCALEPACK, SORTAV*; Nonius: Delft, The Netherlands, 1998.

(25) Sheldrick, G. M. *SHELXS-97*; University of Göttingen: Göttingen, Germany. Windows version by Mc Ardle, Natl. Univ.: Ireland, Galway, 1997.

(26) Sheldrick, G. M. *Acta Crystallogr.* **2008**, *A64*, 112–122.

(27) Farrugia, L. J. *J. Appl. Crystallogr.* **1999**, *32*, 837–838.

(28) Johansson, A.; Ljung, H.; Westman, S. *Acta Shem. Scand.* **1968**, *22*, 2743–2753.

(29) Pu, Z.; Ito, K.; Schleyer, P.v.R.; Li, Q. *Inorg. Chem.* **2008**, *48*, 10679–10686.

(30) Rundqvist, S.; Pramatus, S. *Acta Chem. Scand.* **1967**, *21*, 191–194.

(31) Rogl, P. *Borides with Boron Chains, in Inorganic Reactions and Methods: Formation of Bonds to Group-I, -II, and -IIIB Elements*; Zuckerman, J. J., Hagen, A. P., Eds.; John Wiley & Sons, Inc.: Hoboken, NJ, 1991; Vol. 13.

(32) Ade, M.; Kotzot, D.; Hillebrecht, H. *J. Solid State Chem.* **2010**, *183*, 1790–1797.

(33) Rogl, P.; Nowotny, H. *Monatsh. Chem.* **1973**, *104*, 1325–1332.

(34) Kotzot, D.; Ade, M.; Hillebrecht, H. *Solid State Sci.* **2008**, *10*, 291–302.

(35) Moreau, J. M.; Paccard., D.; Parthé, E. *Acta Crystallogr.* **1974**, *B30*, 2583–2586.

(36) Parthé, E.; Gelato, L.; Chabot, B.; Penzo, M.; Censual, K.; Gladyshevskii, R. *TYPIX—Standardized Data and Crystal Chemical Characterization of Inorganic Structure Types*; Berlin: Springer, 1994.